



## OPEN ACCESS

## EDITED BY

Huili Ma,  
Nanjing Tech University, China

## REVIEWED BY

Wen-Cheng Chen,  
Guangdong University of Technology,  
China  
Zhongjie Ren,  
Beijing University of Chemical  
Technology, China

## \*CORRESPONDENCE

Jian Wang,  
wangjian@cqnu.edu.cn

## SPECIALTY SECTION

This article was submitted to Theoretical and Computational Chemistry, a section of the journal Frontiers in Chemistry

RECEIVED 03 August 2022

ACCEPTED 08 September 2022

PUBLISHED 29 September 2022

## CITATION

Wang J (2022), High efficient room temperature phosphorescent materials constructed with methylene molecular configuration.  
*Front. Chem.* 10:1010676.  
doi: 10.3389/fchem.2022.1010676

## COPYRIGHT

© 2022 Wang. This is an open-access article distributed under the terms of the [Creative Commons Attribution License \(CC BY\)](https://creativecommons.org/licenses/by/4.0/). The use, distribution or reproduction in other forums is permitted, provided the original author(s) and the copyright owner(s) are credited and that the original publication in this journal is cited, in accordance with accepted academic practice. No use, distribution or reproduction is permitted which does not comply with these terms.

# High efficient room temperature phosphorescent materials constructed with methylene molecular configuration

Jian Wang\*

School of Elementary Education, Chongqing Normal University, Chongqing, China

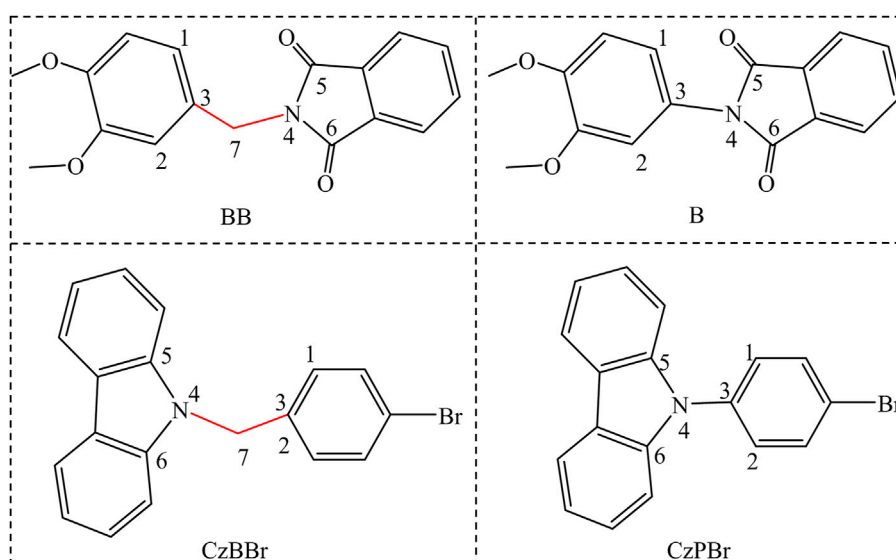
In this work, we have investigated several pure organic room temperature phosphorescent materials with donor-methylene acceptor configurations with relatively different quantum efficiency. The results show that the introduction of methylene functional group in room temperature phosphorescent materials based on donor-acceptor configuration is more favorable for obtaining higher phosphorescent quantum efficiency in crystal phase environment. More importantly, our calculations reveal the root cause of the excellent quantum efficiency performance after the introduction of methylene groups. The results show that the introduction of methylene can inhibit the structural deformation of molecules during the excited state transition process and give them higher interaction. Moreover, in the donor-acceptor configuration, the heavy atom effect is more favorable to the formation of  $\pi$ -x (X = Br) interaction to accelerate the occurrence of intersystem crossing and achieve a higher intersystem crossing rate. Therefore, the donor-methylene-acceptor molecule is expected to improve the quantum efficiency of room temperature phosphorescence, and the addition of heavy atoms is more conducive to prolong the life of room temperature phosphorescence. This work provides a useful reference for rational design of room temperature phosphorescent materials with high efficiency and long life.

## KEYWORDS

room temperature phosphorescent, DFT, methylene, luminescence mechanism, nonradiative rates

## Introduction

Room temperature phosphorescence (RTP) is a luminescent phenomenon different from fluorescence. It has attracted considerable interests due to their fundamental importance and potential applications in optoelectronics, sensors as well as bioimaging. (Baldo et al., 1998; Mi et al., 2010; You et al., 2011; Zhao et al., 2011) It is well known that fluorescent materials can only have a maximum exciton utilization rate of 25%. Therefore, people will turn their attention to phosphorescent materials with higher utilization rate. Early phosphorescent materials were composed of heavy metal complexes. (Ding et al., 2021; Liu et al., 2021; Zhang et al., 2021) Due to



**SCHEME 1**  
The structure of studied molecules.

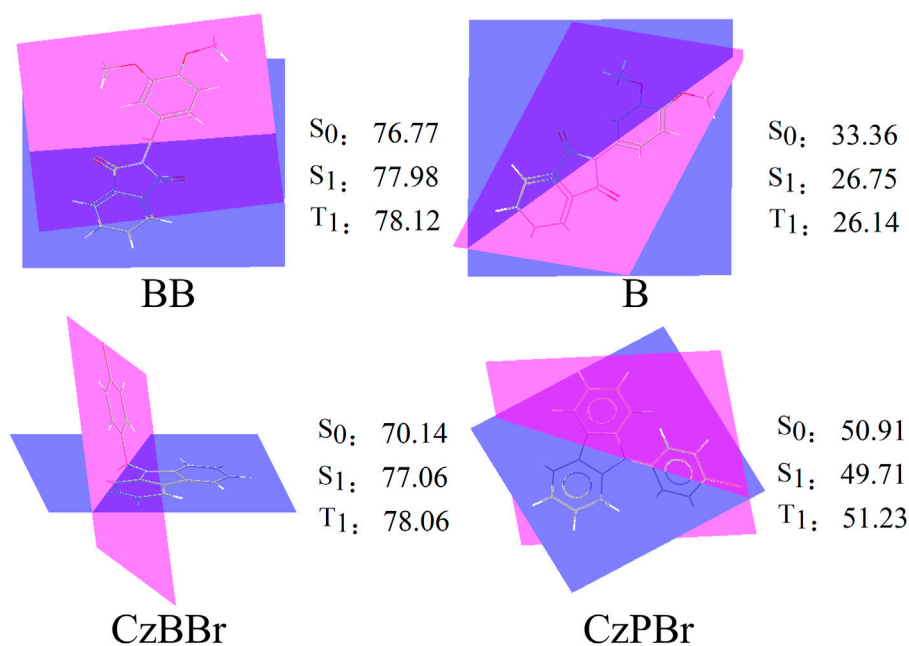
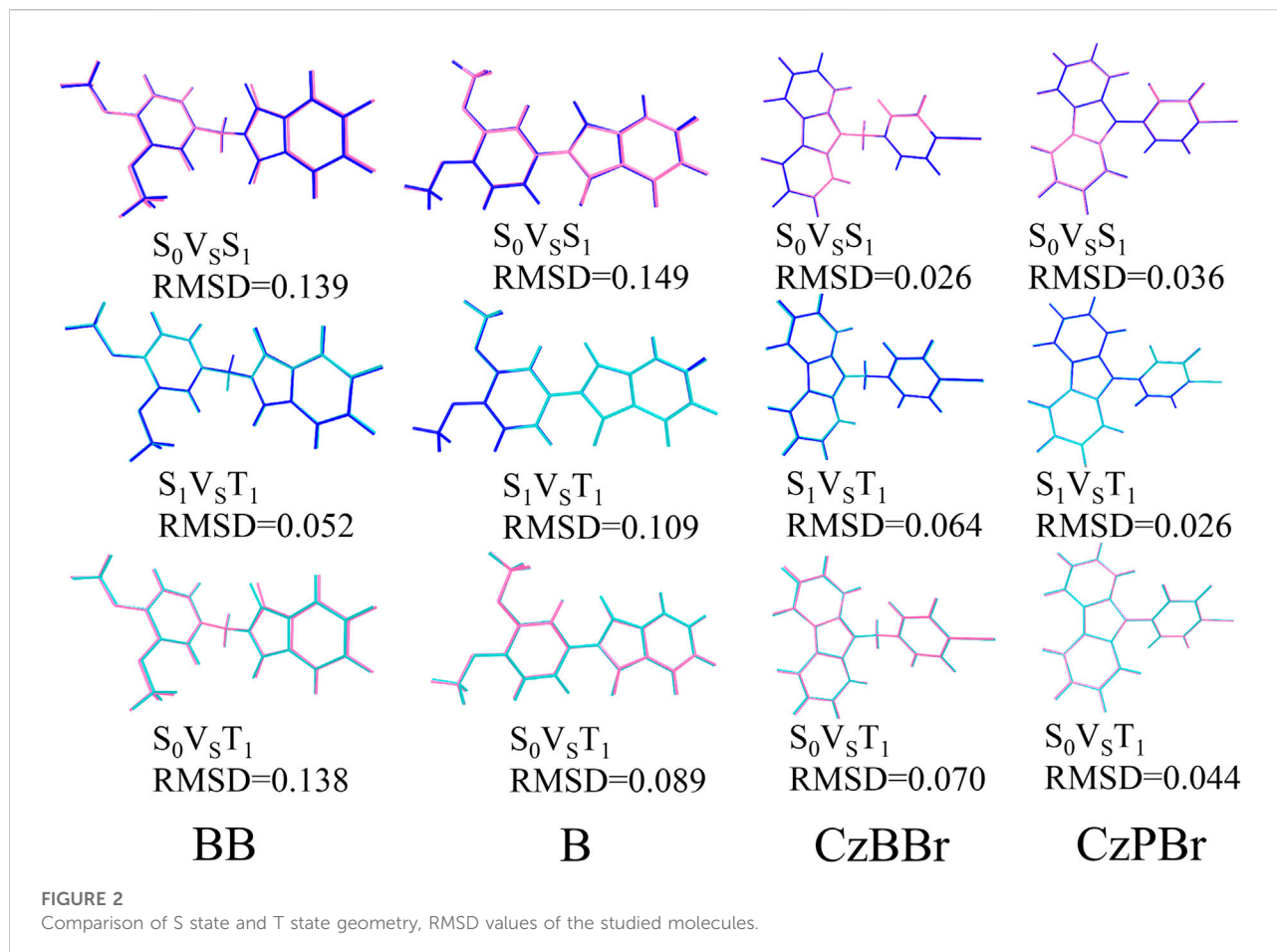


**FIGURE 1**  
The dihedral Angle of studied molecules.

the disadvantages of heavy metal complexes such as high toxicity, high price and instability, more and more researchers turn to room-temperature phosphorescence (RTP) materials with low cost, molecular diversity, high

energy utilization in excited state and long life. (Zhang et al., 2016; Li et al., 2017; Cai et al., 2019a; Cai et al., 2019b; Luo et al., 2019; Zhao et al., 2019; Zhao et al., 2020) However, achieving efficient room temperature phosphorescent

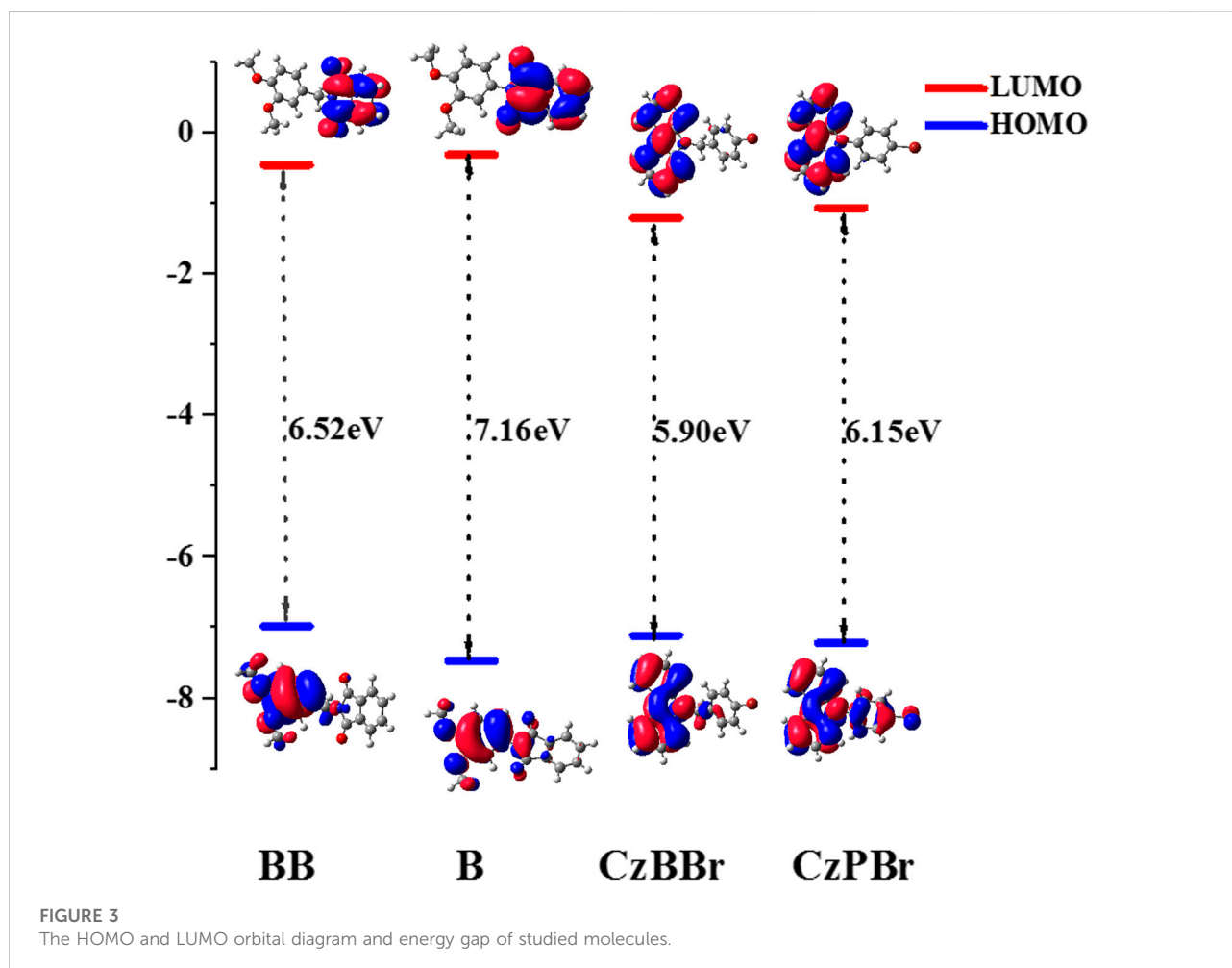


emission in pure organic molecules is a huge challenge due to the instability of triplet exciton and the inefficient intersystem crossing (ISC) process caused by weak spin-orbit coupling (SOC). (Xiong et al., 2018; Lin et al., 2020; Ma et al., 2021).

The ideal high efficiency and long life RTP materials can be defined as: 1) the molecular structure should have the ability to promote intersystem crossing from the single excited state to the triplet excited state, among which halogen and carbonyl groups are the most commonly used; 2) the molecule has an inherently rigid structure or is in a solid-state environment to reduce non-radioactive decay rates, inherently rigid structure usually means having conjugated aromatic rings; 3) Enhance the stability of triplet excitons through intermolecular coupling, face-to-face stacking structures with strong  $\pi$ - $\pi$  interactions are generally considered to be one of the most favorable stacking methods. Compounds with carbonyl groups and conjugated aromatic rings are often used in room temperature phosphorescent materials because of their rigid structures that facilitate efficient intersystem crossing processes. For example, n-electron functional groups (such as aldehyde and carbonyl groups) are

introduced in  $\pi$ -conjugated organic molecules to promote the intersystem crossing. (Pan et al., 2018; Wang et al., 2019; Li et al., 2020) These compounds have strong electron-coupled donor-acceptor skeletons, which tend to cause structural deformation during the excited state transition process, resulting in limited inhibition of molecular motion, or even inhibited by rigid environment. These rigid environments include polymerization, (Su et al., 2020; Wu et al., 2020) host-guest doping, (Lee et al., 2019; Zhang et al., 2019) self-assembly, (Gu et al., 2020; Zhang et al., 2020) crystallization, (Yang et al., 2020) etc. Therefore, the development of organic RTP with high efficiency and long life is a work worth exploring.

In the field of RTP materials, researchers have proposed a RTP material which is connected by methylene. Zhang et al. synthesized and characterized aggregation-induced emission with long-lived room temperature phosphorescence from methylene-linked organic donor-acceptor molecules. (Cai et al., 2018) Due to methylene, the molecule has a tetrahedron-like structure, which is conducive to the formation of a strong intermolecular interaction in the crystal



phase, and can break the electron delocalization between donor and acceptor, and prevent the structural deformation of the excited state transition. In the previous work, we discussed room temperature phosphorescence of methylene linked organic donor-acceptor molecules synthesized and characterized by Zhang et al., under different environments. (Zhao et al., 2021).

Recently, Zhongfu An et al. achieved a phosphorescent quantum efficiency of 39.76% and a phosphorescent lifetime of 220.24 ms by introducing methylene and halogen functional groups into the donor-accepter structures to control structural deformation. (Yin et al., 2020) In addition, halogenated receptors can form intermolecular  $\pi$ -halogen interactions in crystals, accelerating ISC transitions without shortening RTP lifetimes. These experimental studies show that the introduction of methylene between donor and recipient has a profound effect on achieving efficient room temperature phosphorescence. However, how methylene regulate the properties of long-lived room temperature phosphorescence is not well understood.

To further understand the luminescence mechanism, based on BB and CzBBR molecules synthesized by An et al., we designed B molecules without methylene and CzPBr molecules containing halogens without methylene, as shown in Scheme 1. In this work, we use density functional theory to study the electronic structure properties of molecules, ONIOM model to simulate the crystal phase environment, and independent gradient model (IGM) method to analyze the interaction between molecules, hoping to clearly understand the essence of efficient room temperature phosphorescence. The radiative rate, non-radiative rate and intersystem crossing rate of all molecules were evaluated by quantitative calculation. We hope that these results can systematically elucidate the luminescence mechanism of donor-methylene-receptor or donor-methylene-halogenated receptor structures under solid phase conditions, so as to provide theoretical guidance for the preparation of efficient room temperature phosphorescent materials in experiments.

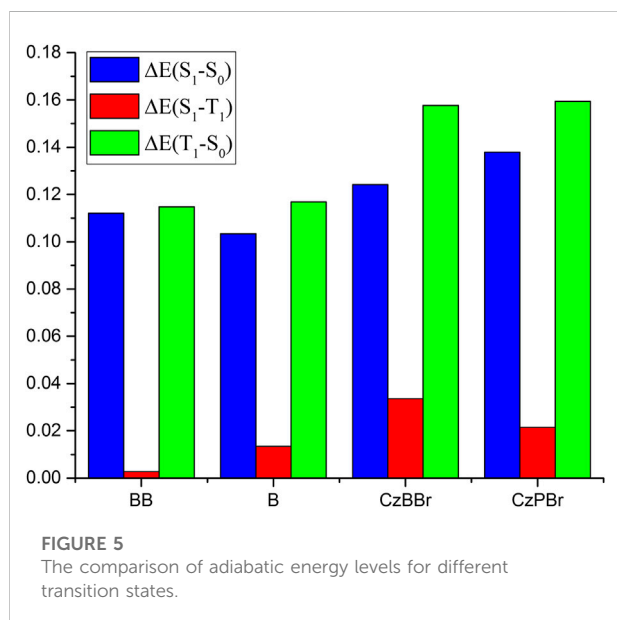
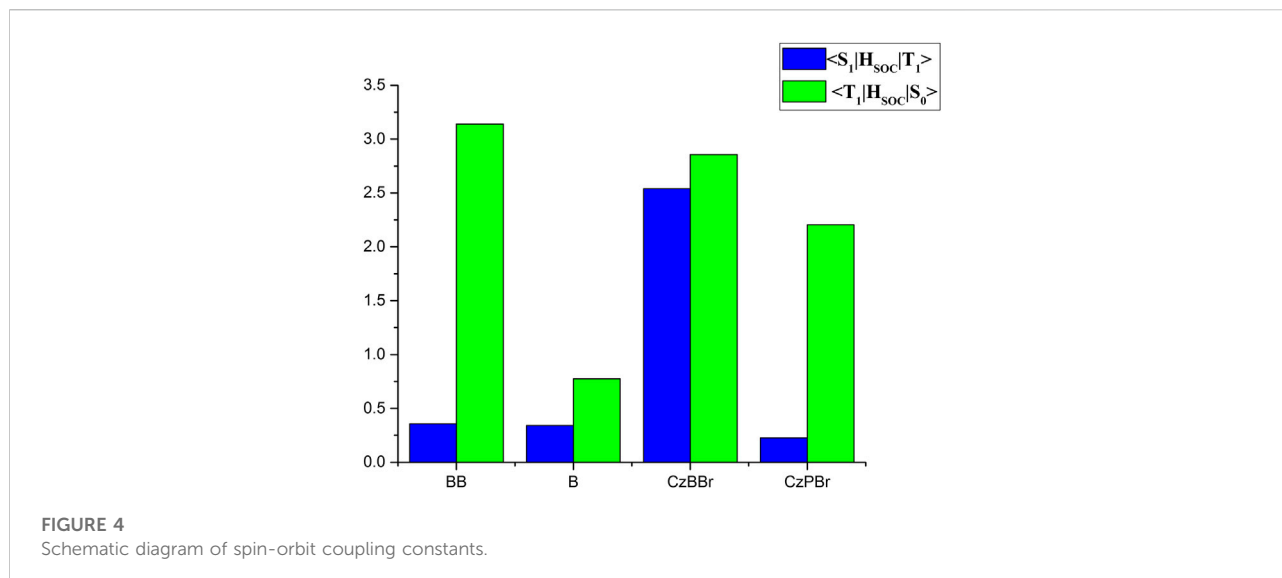


**TABLE 1** The excited state energy (eV) and energy gap (eV) of the studied molecule.

	BB	B	CzBBr	CzPBr
$S_1$	3.12	3.18	4.29	4.34
$T_1$	3.05	2.81	3.38	3.75
$\Delta E(S_1 - T_1)$	0.07	0.37	0.91	0.59

results, we found that the space group of molecule B was P21/C, so we randomly selected one of them as the central molecule to construct ONIOM model. The crystal structures of other molecules were extracted from the Cambridge Crystal Database. The ONIOM model was used for QM/MM calculation, in which the central molecule was defined as the QM part and regarded as the high level, while the surrounding MM part was defined as the low level, and the molecules in the MM region were frozen during the frequency calculation. In the QM/MM calculation, the partial charge of atoms generated by restricted electrostatic potential (RESP) fitting method is used. The above calculation is obtained by using Gaussian 16. (Bredas et al., 2004; Frisch et al., 2016) The structural changes root-mean-square deviation (RMSD) of  $S_0$  and  $T_1$  states,  $S_0$  and  $S_1$  states and  $S_1$  and  $T_1$  states were calculated by VMD program. (Humphrey et al., 1996) The donor-acceptor dihedral Angle was obtained by Mercury program analysis. (Macrae et al., 2006) The spin orbit coupling (SOC) matrix elements between  $T_1$  and  $S_0$  states and between  $T_1$  and  $S_1$  are calculated using the quadratic response theory by Dalton 2016 program. (K et al., 2014; Vahtras et al., 1992) The Multiwfn program was used to calculate the natural transition orbits, and analyze the transition properties of molecules. (Lu and Chen, 2012) IGM method was used to visualize the interaction between

## Computational method

All molecules were structurally optimized at the  $\omega$ B97XD/6-31g\*\* level. Based on the optimized geometry, the frequencies of all molecules were calculated, and all frequencies had no virtual frequency to confirm that these structures were the lowest point in the potential energy surface. The crystal structure of molecule B were predicted by universal force field (UFF) by Polymorph module. (Rappe et al., 1993; Akkermans et al., 2013) We selected the five most probable space groups (P21/C, P2121, P1, P21, P1) and calculated by extracting the crystal structure of the space group with the lowest energy. By comparing the calculation

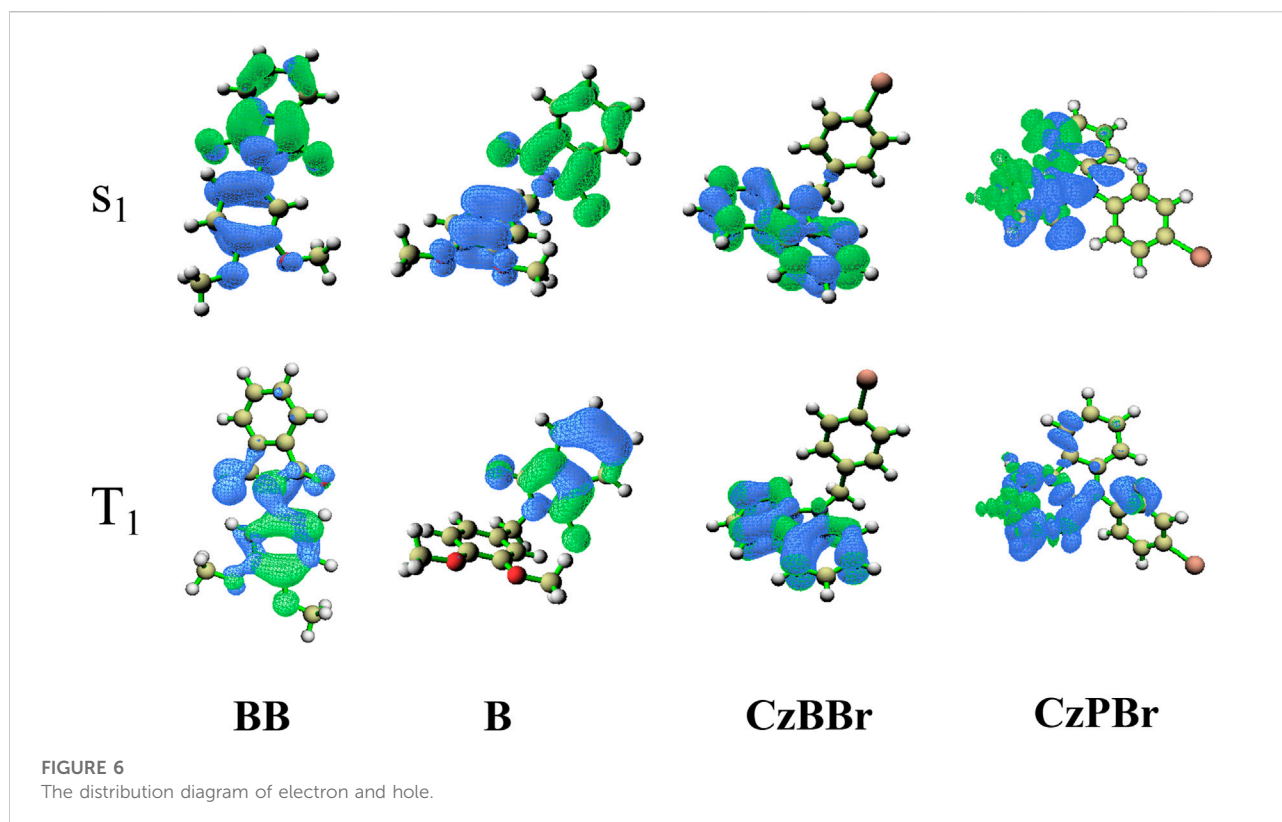


TABLE 2 The optical physical property parameters of studied molecules.

	$S_1 \rightarrow T_1$	$T_1 \rightarrow S_0$		$\Phi_p$ (%)	
	$k_{isc}$ ( $s^{-1}$ )	$K_r$ ( $s^{-1}$ )	$k_{nr}$ ( $s^{-1}$ )	calcd	exptl
BB	$1.87 \times 10^8$	52.6	$1.20 \times 10^3$	4.2	3.5
B	$1.32 \times 10^5$	1.66	$9.07 \times 10^3$		
CzBBr	$3.29 \times 10^8$	0.16	$1.12 \times 10^2$		
CzPBr	$8.87 \times 10^4$	0.26	0.51		

molecules. (Lefebvre et al., 2017) Based on the data obtained above, MOMAP program was used to perform frequency analysis and calculate the intersystem crossing rate, radiative rate and non-radiative rate. (Niu et al., 2018).

## Results and discussion

### Structure of ground state and excited state

The geometrical and electronic structures of molecules play an important role in the photophysical properties, thus determining the luminescence efficiency of organic molecules. To investigate the effect of methylene and heavy atom effects on

molecular structure, we calculated the dihedral Angle between donor and acceptor, as shown in Figure 1. In general, the dihedral Angle can reflect the degree of structural distortion of the material molecules. The dihedral angles of singlet S0 and first excited triplet T1 of BB are  $76.77^\circ$  and  $78.12^\circ$ , and the variation between them is less than that of molecule B (the dihedral angles of S0 and T1 states of molecule B are  $33.36^\circ$  and  $26.14^\circ$ ). This indicates that the introduction of methylene is beneficial to inhibit molecular structural deformation. However, the dihedral angles of CzBBr and CzPBr are different. The dihedral angles of CzBBr in S0 and T1 states are  $70.14^\circ$  and  $78.06^\circ$ , and the dihedral angles of CzPBr in S0 and T1 states are  $50.91^\circ$  and  $51.23^\circ$ , respectively. The variation of dihedral Angle for S0 and S1 is consistent with that of S0 and T1. This indicates that the introduction of heavy atoms and methylene group has counteracting effect on the structural deformation. In order to quantitatively characterize the structural deformation during electron transition, we calculate the root mean square displacement (RMSD).

$$RMSD = \sqrt{\frac{1}{N} \sum_i^{natom} [(X_i - X'_i)^2 + (Y_i - Y'_i)^2 + (Z_i - Z'_i)^2]}$$

The changes and RMSD values between S0, S1 and T1 states of all molecules are shown in Figure 2. RMSD values of S0 vs. S1, S1 vs. T1 and S0 vs. T1 of molecular BB were 0.139, 0.052, 0.138, respectively. The RMSD values of S0 vs. S1, S1 vs. T1 and S0 vs. T1 states of molecule B are 0.149, 0.109 and 0.089 respectively,



indicating that the degree of structural distortion of molecule B is greater than that of molecule BB, which is consistent with the change of dihedral Angle discussed above. From the above analysis, it can be seen that the introduction of methylene and heavy atoms can cause geometrical changes of molecules, which may have a significant effect on the excited state properties of molecules.

## Energy level and transition properties

To explore the electrical properties of molecules, the HOMO and LUMO levels of all molecules are calculated. As shown in Figure 3, the HOMO level of both BB and CzBBr molecules introduced with methylene is higher than that of B and CzPBr molecules without methylene. The results indicate that the introduction of methylene and heavy atom play an important role in the transition properties of molecules. It can be clearly seen from Figure 3 that the HOMO wave functions of BB and CzBBr molecules are mainly distributed on the donor, while the HOMO of B and CzPBr molecules are delocalized toward the acceptor. For LUMO, BB and B molecules are mainly distributed on the acceptor, while CzBBr and CzPBr molecules are mainly distributed on the donor unit.

The SOC between S1 and T1 states and between S0 and T1 states for studied molecules are illustrated in Figure 4. As shown in Figure 4 the SOC value between S1 and T1 states of CzBBr molecule ( $2.54 \text{ cm}^{-1}$ ) was greater than CzPBr molecule ( $0.23 \text{ cm}^{-1}$ ). For BB molecule and B molecule, there is little difference in SOC between them, which may be due to the absence of heavy atom effect. This indicates that CzBBr molecule has a faster ISC rate between S1 and T1 than CzPBr molecule, while BB and B molecule have similar ISC rates. Phosphorescent quantum efficiency and lifetime are two important parameters to evaluate the performance of RTP molecules. To calculate these two quantities, we optimized the excited states and calculated  $\Delta E_{(S_1-T_1)}$ . As shown in Figure 5 and Table 1, the molecular BB, B, CzBBr and CzPBr were 0.07, 0.37, 0.91 and 0.59 eV, respectively.

It is worth noting that the energy difference of CzBBr molecule is the largest, which indicates that CzBBr molecule may have a small intersystem crossing rate, but this is contrary to the experimental value. The reason is that the SOC value between S1 and T1 states of CzBBr is large, which leads to a large intersystem channelage rate. This is consistent with the intersystem crossing rate calculated theoretically in the following paper. Similarly, the trend of  $\Delta E_{(T_1-S_0)}$  is opposite to that of  $\Delta E_{(S_1-T_1)}$ , which may be caused by the different oscillator strength of  $T_1 \rightarrow S_0$  (the oscillator strength of BB, B, CzBBr and CzPBr are  $1.67 \times 10^{-8}$ ,  $1.74 \times 10^{-10}$ ,  $9.64 \times 10^{-11}$ ,  $6.76 \times 10^{-11}$ , respectively). In order to better explore the emission state properties, the electron hole distribution based on the first

excited triplet state are calculated. As shown in Figure 6, compared with molecules B and CzPBr without methylene introduced, the T1 states of molecules BB and CzBBr are locally excited in the donor unit, while molecule B is locally excited in the acceptor unit, and the S1 states of molecules BB and B are charge transfer states distributed in the whole molecule. This shows that the nature of the excited states are changed along with the introduction of methylene and heavy atoms. Therefore, the introduction of methylene and heavy atoms is invaluable for the construction of efficient RTP.

## Radiative and nonradiative rates

In order to further explore the radiation situation, the calculated photophysical parameter of all molecules are listed in Table 2. As shown in Table 2, the intersystem crossing constants  $k_{isc(S_1-T_1)}$  of BB and CzBBr molecules with methylene group introduced are larger than those of B and CzPBr molecules without methylene group introduced, which is consistent with the orbital coupling and energy difference discussed above. In addition, the radiation rate constant ( $k_r$ ) of BB is increased from 1.66 to  $52.6 \text{ s}^{-1}$ , and has the maximum value in selected molecules, due to the enhanced spin coupling value  $H_{SOC}$ . It is noteworthy that the calculated phosphorescent quantum efficiency is in good agreement with the experimental value, which also proves the reliability of our calculation method.

## Conclusion

In this work, we investigate two kinds of donor-methylene-acceptor and donor-acceptor pure organic room temperature phosphorescent materials with relatively different quantum efficiency. The results show that the introduction of methylene functional group in room temperature phosphorescent materials based on donor-acceptor configuration is more favorable for obtaining higher phosphorescent quantum efficiency in crystal phase environment. The results show that the introduction of methylene functional groups in room temperature phosphorescent materials can inhibit the molecular structural deformation during the excited state transition process, and can give it higher intermolecular interaction, which is more conducive to obtain higher phosphorescent quantum efficiency in crystal phase environment. In addition, the heavy atom effect is more favorable to the formation of  $\pi$ -x (X = Br) interaction in the donor-acceptor configuration, resulting in higher intersystem crossing rate. Therefore, the introduction of methylene and heavy atoms into donor-acceptor materials is expected to improve the quantum efficiency of room temperature phosphorescence and prolong the life of room temperature phosphorescence, which provides a new strategy for rational

design of high efficiency and long life of room temperature phosphorescence materials.

## Data availability statement

The original contributions presented in the study are included in the article/supplementary material, further inquiries can be directed to the corresponding author.

## Author contributions

The author confirms being the sole contributor of this work and has approved it for publication.

## References

- Akkermans, R. L. C., Spenley, N. A., and Robertson, S. H. (2013). Monte Carlo methods in materials studio. *Mol. Simul.* 39 (14–15), 1153–1164. doi:10.1080/08927022.2013.843775
- Baldo, M. A., O'Brien, D. F., You, Y., Shoustikov, A., and Sibley, S., (1998). Highly efficient phosphorescent emission from organic electroluminescent devices. *Nature* 395 (6698), 151–154. doi:10.1038/25954
- Bredas, J. L., Beljonne, D., Coropceanu, V., and Cornil, J. (2004). Charge-transfer and energy-transfer processes in pi-conjugated oligomers and polymers: A molecular picture. *Chem. Rev.* 104 (11), 4971–5004. doi:10.1021/cr040084k
- Cai, S., Shi, H., Tian, D., Ma, H., and Cheng, Z. (2018). Organic phosphorescence: Enhancing ultralong organic phosphorescence by effective  $\pi$ -type halogen bonding (adv. Funct. Mater. 9/2018). *Adv. Funct. Mater.* 28 (9), 1870060. doi:10.1002/adfm.201870060
- Cai, W., Zhang, H., Yan, X., Zhao, A., and He, R., (2019). What accounts for the color purity of tetradentate Pt complexes? A computational analysis. *Phys. Chem. Chem. Phys.* 21 (15), 8073–8080. doi:10.1039/c9cp00819e
- Cai, W., Zhao, A., Ren, K., He, R., Li, M., and Shen, W. (2019). Understanding the mechanisms of white light emission of a tetradentate Pt complex in various surrounding environments. *J. Phys. Chem. C* 123 (29), 17968–17975. doi:10.1021/acs.jpcc.9b04217
- Ding, B., Gao, H., Wang, C., and Ma, X. (2021). Reversible room-temperature phosphorescence in response to light stimulation based on a photochromic copolymer. *Chem. Commun.* 57, 3154–3157. doi:10.1039/d1cc00613d
- Frisch, M. J., Trucks, G. W., Schlegel, H. B., Scuseria, G. E., and Robb, M. A., (2016). *Gaussian 16*. Wallingford, CT: Rev. B.01.
- Gu, L., Wu, H., Ma, H., Ye, W., and Jia, W., (2020). Color-tunable ultralong organic room temperature phosphorescence from a multicomponent copolymer. *Nat. Commun.* 11 (1), 944–948. doi:10.1038/s41467-020-14792-1
- Humphrey, W., Dalke, A., and Schulten, K. (1996). Vmd: Visual molecular dynamics. *J. Mol. Graph.* 14 (1), 33–38. doi:10.1016/0263-7855(96)00018-5
- Kestutis, A., Celestino, A., Keld, B., Vebjørn, B., and Radovan, B. (2014). Dalton quantum Chem. program Syst, *Wiley Interdiscip Rev Comput Mol Sci*, 4 (3), 269–284. doi:10.1002/wcms.1172
- Lee, D. R., Han, S. H., and Lee, J. Y. (2019). Metal-free and purely organic phosphorescent light-emitting diodes using phosphorescence harvesting hosts and organic phosphorescent emitters. *J. Mat. Chem. C Mat.* 7 (37), 11500–11506. doi:10.1039/c9tc03203g
- Lefebvre, C., Rubez, G., Khartabil, H., Boisson, J. C., Contreras-Garcia, J., and Henon, E. (2017). Accurately extracting the signature of intermolecular interactions present in the NCI plot of the reduced density gradient versus electron density. *Phys. Chem. Chem. Phys.* 19 (27), 17928–17936. doi:10.1039/c7cp02110k
- Li, H., Li, H., Wang, W., Tao, Y., Wang, S., and Yang, Q., (2020). Stimuli-responsive circularly polarized organic ultralong room temperature phosphorescence. *Angew. Chem. Int. Ed. Engl.* 132 (12), 4786–4792. doi:10.1002/ange.201915164
- Li, W., Peng, Q., Ma, H., Wen, J., Ma, J., and Peteanu, L. A., (2017). Theoretical investigations on the roles of intramolecular structure distortion versus irregular intermolecular packing in optical spectra of 6T nanoparticles. *Chem. Mat.* 29 (6), 2513–2520. doi:10.1021/acs.chemmater.6b04210
- Lin, Z., Kabe, R., Wang, K., and Adachi, C. (2020). Influence of energy gap between charge-transfer and locally excited states on organic long persistence luminescence. *Nat. Commun.* 11 (1), 191–197. doi:10.1038/s41467-019-14035-y
- Liu, J., Ma, Z., Li, Z., Liu, Y., Fu, X., and Jiang, H., (2021). Room-temperature white and color-tunable afterglow by manipulating multi-mode triplet emissions. *J. Mat. Chem. C Mat.* 9 (9), 3257–3263. doi:10.1039/d0tc05816e
- Lu, T., and Chen, F. (2012). Multiwfn: A multifunctional wavefunction analyzer. *J. Comput. Chem.* 33 (5), 580–592. doi:10.1002/jcc.22885
- Luo, Y., Chen, Z., Hu, J., Xu, Z., Meng, Q., and Tang, D. (2019). Small substituent groups as geometric controllers for tridentate platinum(ii) complexes to effectively suppress non-radiative decay processes. *Phys. Chem. Chem. Phys.* 21 (5), 2764–2770. doi:10.1039/c8cp06804f
- Ma, X., Jia, L., Yang, B., Li, J., Huang, W., and Wu, D., (2021). A color-tunable single molecule white light emitter with high luminescence efficiency and ultra-long room temperature phosphorescence. *J. Mat. Chem. C Mat.* 9 (2), 727–735. doi:10.1039/d0tc04234j
- Macrae, C. F., Edgington, P. R., McCabe, P., Pidcock, E., Shields, G. P., and Taylor, R., (2006). Mercury: Visualization and analysis of crystal structures. *J. Appl. Crystallogr.* 39, 453–457. doi:10.1107/s002188980600731x
- Mi, B. X., Gao, Z. Q., Liao, Z. J., Huang, W., and Chen, C. H. (2010). Molecular hosts for triplet emitters in organic light-emitting diodes and the corresponding working principle. *Sci. China Chem.* 53 (8), 1679–1694. doi:10.1007/s11426-010-4043-7
- Niu, Y. L., Li, W. Q., Peng, Q., Geng, H., Yi, Y. P., and Wang, L. J., (2018). MOlecular MAterials property prediction package (MOMAP) 1.0: A software package for predicting the luminescent properties and mobility of organic functional materials. *Mol. Phys.* 116 (7–8), 1078–1090. doi:10.1080/00268976.2017.1402966
- Pan, S., Chen, Z., Zheng, X., Wu, D., Chen, G., and Xu, J., (2018). Ultralong room-temperature phosphorescence from supramolecular behavior via intermolecular electronic coupling in pure organic crystals. *J. Phys. Chem. Lett.* 9 (14), 3939–3945. doi:10.1021/acs.jpcclett.8b01697
- Rappe, A. K., Colwell, K. S., and Casewit, C. J. (1993). Application of a universal force-field to metal-complexes. *Inorg. Chem.* 32 (16), 3438–3450. doi:10.1021/ic00068a012
- Su, Y., Zhang, Y., Wang, Z., Gao, W., Jia, P., and Zhang, D., (2020). Excitation-dependent long-life luminescent polymeric systems under ambient conditions. *Angew. Chem. Int. Ed. Engl.* 59 (25), 10053–10057. doi:10.1002/ange.201912102
- Vahtras, O., Agren, H., Jorgensen, P., Jensen, H. J. A., Helgaker, T., and Olsen, J. (1992). Multiconfigurational quadratic response functions for singlet and triplet perturbations the phosphorescence lifetime of formaldehyde. *J. Chem. Phys.* 97 (12), 9178–9187. doi:10.1063/1.463344

## Conflict of interest

The author declares that the research was conducted in the absence of any commercial or financial relationships that could be construed as a potential conflict of interest.

## Publisher's note

All claims expressed in this article are solely those of the authors and do not necessarily represent those of their affiliated organizations, or those of the publisher, the editors and the reviewers. Any product that may be evaluated in this article, or claim that may be made by its manufacturer, is not guaranteed or endorsed by the publisher.



- Wang, T., Su, X., Zhang, X., Nie, X., Huang, L., and Zhang, X., (2019). Aggregation-induced dual-phosphorescence from organic molecules for nondoped light-emitting diodes. *Adv. Mat.* 31 (51), 1904273. doi:10.1002/adma.201904273
- Wu, H., Gu, L., Baryshnikov, G. V., Wang, H., Minaev, B. F., and Ågren, H., (2020). Molecular phosphorescence in polymer matrix with reversible sensitivity. *ACS Appl. Mat. Interfaces* 12 (18), 20765–20774. doi:10.1021/acsami.0c04859
- Xiong, Y., Zhao, Z., Zhao, W., Ma, H., Peng, Q., and He, Z., (2018). Designing efficient and ultralong pure organic room-temperature phosphorescent materials by structural isomerism. *Angew. Chem. Int. Ed. Engl.* 130 (27), 8129–8133. doi:10.1002/ange.201800834
- Yang, Z., Ubba, E., Huang, Q., Mao, Z., Li, W., and Chen, J., (2020). Enabling dynamic ultralong organic phosphorescence in molecular crystals through the synergy between intramolecular and intermolecular interactions. *J. Mat. Chem. C Mat.* 8 (22), 7384–7392. doi:10.1039/d0tc00975j
- Yin, Z., Gu, M., Ma, H., Jiang, X., Zhi, J., and Wang, Y., (2020). Molecular engineering through control of structural deformation for highly efficient ultralong organic phosphorescence. *Angew. Chem. Int. Ed. Engl.* 59, 2086–2091. doi:10.1002/ange.202011830
- You, Y., Lee, S., Kim, T., Ohkubo, K., Chae, W. S., and Fukuzumi, S., (2011). Phosphorescent sensor for biological mobile zinc. *J. Am. Chem. Soc.* 133 (45), 18328–18342. doi:10.1021/ja207163r
- Zhang, T., Ma, X., Wu, H., Zhu, L., Zhao, Y., and Tian, H. (2020). Molecular engineering for metal-free amorphous materials with room-temperature phosphorescence. *Angew. Chem. Int. Ed. Engl.* 59 (28), 11302–11312. doi:10.1002/ange.201915433
- Zhang, T., Wu, Y., and Ma, X. (2021). Tunable multicolor room-temperature phosphorescence including white-light emission from amorphous copolymers. *Chem. Eng. J.* 412, 128689. doi:10.1016/j.cej.2021.128689
- Zhang, W., Luo, Y., Xu, Y., Li, W., and Shen, W. (2016). Theoretical investigation and design of highly efficient blue phosphorescent iridium(III) complexes bearing fluorinated aromatic sulfonyl groups. *ChemPhysChem* 17 (24), 4149–4157. doi:10.1002/cphc.201600945
- Zhang, Z. Y., Chen, Y., and Liu, Y. (2019). Efficient room-temperature phosphorescence of a solid-state supramolecule enhanced by cucurbit [6] uril. *Angew. Chem. Int. Ed. Engl.* 131 (18), 6089–6093. doi:10.1002/ange.201901882
- Zhao, A., Cai, W., Yan, X., Zhang, H., Wang, J., and Shen, W. (2019). Theoretical insights into the effect of ligands on platinum(II) complexes with a bidentate bis(o-carborane) ligand structure. *Photochem. Photobiol. Sci.* 18 (10), 2421–2429. doi:10.1039/c9pp00251k
- Zhao, A. C., Cai, W. L., Wu, X. L., and Shen, W. (2020). Unveiling the relationship between the phosphorescent quantum yield and structural modification to construct high-performance Pt(II) complex. *Inorg. Chim. Acta* 512, 119861. doi:10.1016/j.ica.2020.119861
- Zhao, A., Wu, X., Jiang, X., Gao, J., Wang, J., and Shen, W. (2021). Unveiling the mechanisms of organic room temperature phosphorescence in various surrounding environments: A computational study. *Phys. Chem. Chem. Phys.* 23 (47), 26813–26821. doi:10.1039/d1cp03010h
- Zhao, Q., Huang, C., and Li, F. (2011). Phosphorescent heavy-metal complexes for bioimaging. *Chem. Soc. Rev.* 40 (5), 2508–2524. doi:10.1039/c0cs00114g